Inhibition of the glucocorticoid-activating enzyme 11β-hydroxysteroid dehydrogenase type 1 drives concurrent 11-oxygenated androgen excess

Schiffer, Lina; Oestlund, Imken; Snoep, Jacky L.; Gilligan, Lorna C.; Taylor, Angela E.; Sinclair, Alexandra J.; Singhal, Rishi; Freeman, Adrian; Ajjan, Ramzi; Tiganescu, Ana; Arlt, Wiebke; Storbeck, Karl-Heinz

DOI:
10.1096/fj.202302131r

Document Version
Publisher's PDF, also known as Version of record

Citation for published version (Harvard):
Schiffer, L, Oestlund, I, Snoep, JL, Gilligan, LC, Taylor, AE, Sinclair, AJ, Singhal, R, Freeman, A, Ajjan, R, Tiganescu, A, Arlt, W & Storbeck, KH 2024, 'Inhibition of the glucocorticoid-activating enzyme 11β-hydroxysteroid dehydrogenase type 1 drives concurrent 11-oxygenated androgen excess', *FASEB Journal*, vol. 38, no. 7, e23574. https://doi.org/10.1096/fj.202302131r

Received: 19 October 2023 | Revised: 19 February 2024 | Accepted: 11 March 2024

DOI: 10.1096/fj.202302131R

RESEARCH ARTICLE

The FASEB Journal

Inhibition of the glucocorticoid-activating enzyme 11β-hydroxysteroid dehydrogenase type 1 drives concurrent 11-oxygenated androgen excess

Lina Schiffer[1] | **Imken Oestlund**[2] | **Jacky L. Snoep**[2,3] | **Lorna C. Gilligan**[1] | **Angela E. Taylor**[1] | **Alexandra J. Sinclair**[1] | **Rishi Singhal**[4] | **Adrian Freeman**[5] | **Ramzi Ajjan**[6,7] | **Ana Tiganescu**[6,7] | **Wiebke Arlt**[1,8,9] | **Karl-Heinz Storbeck**[1,2]

[1]Institute of Metabolism and Systems Research, University of Birmingham, Birmingham, UK

[2]Department of Biochemistry, Stellenbosch University, Stellenbosch, South Africa

[3]Molecular Cell Biology, Vrije Universiteit Amsterdam, Amsterdam, The Netherlands

[4]Upper GI Unit and Minimally Invasive Unit, Heartlands Hospital, University Hospitals Birmingham NHS Foundation Trust, Birmingham, UK

[5]Emerging Innovations Unit, Discovery Sciences, BioPharmaceuticals R&D, AstraZeneca, Cambridge, UK

[6]Leeds Institute of Cardiovascular and Metabolic Medicine, University of Leeds, Leeds, UK

[7]NIHR Leeds Biomedical Research Center, Leeds Teaching Hospitals, NHS Trust, Leeds, UK

[8]Institute of Clinical Sciences, Faculty of Medicine, Imperial College, London, UK

[9]Medical Research Council Laboratory of Medical Sciences, London, UK

Correspondence
Karl-Heinz Storbeck, Department of Biochemistry, Stellenbosch University, Private Bag X1, Matieland, Stellenbosch 7602, South Africa.
Email: storbeck@sun.ac.za

Funding information
National Research Foundation (NRF), Grant/Award Number: 132503, SRUG2204052159 and 82813; The Academy of Medical Sciences, Grant/Award Number: NAF004\1002; Wellcome Trust (WT), Grant/Award Number: WT209492/Z/17/Z; UKRI | Medical Research Council (MRC), Grant/Award Number: MC_PC_15046

Abstract

Aldo-keto reductase 1C3 (AKR1C3) is a key enzyme in the activation of both classic and 11-oxygenated androgens. In adipose tissue, AKR1C3 is co-expressed with 11β-hydroxysteroid dehydrogenase type 1 (HSD11B1), which catalyzes not only the local activation of glucocorticoids but also the inactivation of 11-oxygenated androgens, and thus has the potential to counteract AKR1C3. Using a combination of in vitro assays and in silico modeling we show that HSD11B1 attenuates the biosynthesis of the potent 11-oxygenated androgen, 11-ketotestosterone (11KT), by AKR1C3. Employing ex vivo incubations of human female adipose tissue samples we show that inhibition of HSD11B1 results in the increased peripheral biosynthesis of 11KT. Moreover, circulating 11KT increased 2–3 fold in individuals with type 2 diabetes after receiving the selective oral HSD11B1

Abbreviations: 11KA4, 11-ketoandrostenedione; 11KT, 11-ketotestosterone; 11OHA4, 11β-hydroxyandrostenedione; 11OHT, 11β-hydroxytestosterone; AKR1C3, aldo-keto reductase 1C3; AR, androgen receptor; CBX, carbenoxolone; DHEAS, dehydroepiandrosterone sulfate; DMEM, Dulbecco's modified Eagle's medium; GC-MS, gas chromatography-mass spectrometry; GR, glucocorticoid receptor; H6PDH, hexose 6-phosphate dehydrogenase; HSD11B1, 11β-hydroxysteroid dehydrogenase type 1; HSD11B2, 11β-hydroxysteroid dehydrogenase type 2; HSS, high strength silica; MASLD, metabolic dysfunction-associated steatotic liver disease; MRM, multiple reaction monitoring; MTBE, Tert-methyl butyl ether; ODE, ordinary differential equations; PCOS, polycystic ovary syndrome; SGBS, Simpson-Golabi-Behmel syndrome; UHPLC-MS/MS, ultra-high performance liquid chromatography tandem mass spectrometry.

Lina Schiffer and Imken Oestlund shared first authors.

inhibitor AZD4017 for 35 days, thus confirming that HSD11B1 inhibition results in systemic increases in 11KT concentrations. Our findings show that HSD11B1 protects against excess 11KT production by adipose tissue, a finding of particular significance when considering the evidence for adverse metabolic effects of androgens in women. Therefore, when targeting glucocorticoid activation by HSD11B1 inhibitor treatment in women, the consequently increased generation of 11KT may offset beneficial effects of decreased glucocorticoid activation.

KEYWORDS

11-ketotestosterone, adipose tissue, aldo-keto reductase 1C3 (AKR1C3), intracrinology, metabolic syndrome

1 | INTRODUCTION

The 11-oxygenated androgens are a group of adrenal-derived and peripherally activated androgens that make a significant contribution to the circulating androgen pool, particularly in women.[1–4] The most potent 11-oxygenated androgen in circulation is 11-ketotestosterone (11KT), which has been shown to bind to and activate the androgen receptor with an affinity and potency similar to testosterone.[5] Moreover, several studies have also shown that 11KT circulates at concentrations equal to or higher than those of testosterone in women.[3,6,7] Unlike the classic androgens, 11-oxygenated androgens do not decline with age, with the result that 11KT is the most abundant active androgen in the circulation of postmenopausal women.[3,6] While the role of 11-oxygenated androgens in healthy individuals has yet to be defined, these androgens have been shown to play a role in disease states such as polycystic ovary syndrome (PCOS), congenital adrenal hyperplasia (CAH), Cushing's syndrome and castration resistant prostate cancer (CRPC).[8–12]

The biosynthesis of 11KT begins in the adrenal, where cytochrome P450 11B1 (CYP11B1) catalyzes the 11β-hydroxylation of locally produced androstenedione to yield 11β-hydroxyandrostenedione (11OHA4). 11OHA4 is released into circulation, and serves as the primary precursor for the biosynthesis of 11KT by peripheral tissues (Figure 1). Specifically, 11OHA4 is converted to 11-ketoandrostenedione (11KA4) by mineralocorticoid target tissues expressing 11β-hydroxysteroid dehydrogenase type 2 (HSD11B2), such as the kidney.[13] 11KA4 then subsequently serves as the substrate for the key androgen activating enzyme, aldo-keto reductase 1C3 (AKR1C3), which is abundantly expressed in adipose tissue.[14–17] Notably, AKR1C3 catalyzes the conversion of 11KA4 to 11KT significantly more efficiently than that of androstenedione to testosterone.[16,17] The biosynthesis of 11KT is, however, more complex than that of testosterone as the presence of the 11-keto group makes both 11KA4 and 11KT substrates for 11β-hydroxysteroid dehydrogenase type 1 (HSD11B1)—an enzyme best known for amplification of glucocorticoid signaling, which it achieves by converting the inactive cortisone to active cortisol in key metabolic tissues including the liver, adipose tissue and skeletal muscle.[11,18–20] Given that AKR1C3 and HSD11B1 are co-expressed in adipose tissue, we propose that HSD11B1 regulates the amount of 11KT produced in two ways. First, by competing with AKR1C3 for 11KA4, thereby limiting the amount of 11KA4 converted to 11KT by AKR1C3. Secondly, by converting some of the 11KT formed to the far less androgenic 11β-hydroxytestosterone (11OHT)[11] (Figure 1). Indeed, while investigating the metabolism of 11KA4 in differentiated Simpson-Golabi-Behmel syndrome preadipocyte (SGBS) cells Paulukinas et al. noted that HSD11B1 may be protective of androgen excess.[17]

This proposed mechanism is important when considering that HSD11B1 has long been a therapeutic target for prevention of tissue-specific excess glucocorticoid exposure and treatment of related adverse metabolic effects.[19,21–24] Promising preclinical studies in rodents, which crucially do not produce 11-oxygenated androgens,[25–30] were unable to accurately model competing HSD11B1 and AKR1C3 effects in humans. Our proposed hypothesis could provide an explanation for the more limited effects observed in clinical trials with HSD11B1 inhibitors,[31–42] as increased 11KT production resulting from HSD11B1 inhibition could counteract beneficial effects of reduced glucocorticoid signaling, by increasing androgen signaling. This is particularly significant in women where elevated androgens are linked to insulin resistance, type 2 diabetes, hypertension, cardiovascular disease and metabolic dysfunction-associated steatotic liver disease (MASLD), in particular in the context of PCOS, for which androgen excess is a defining feature.[43–52]

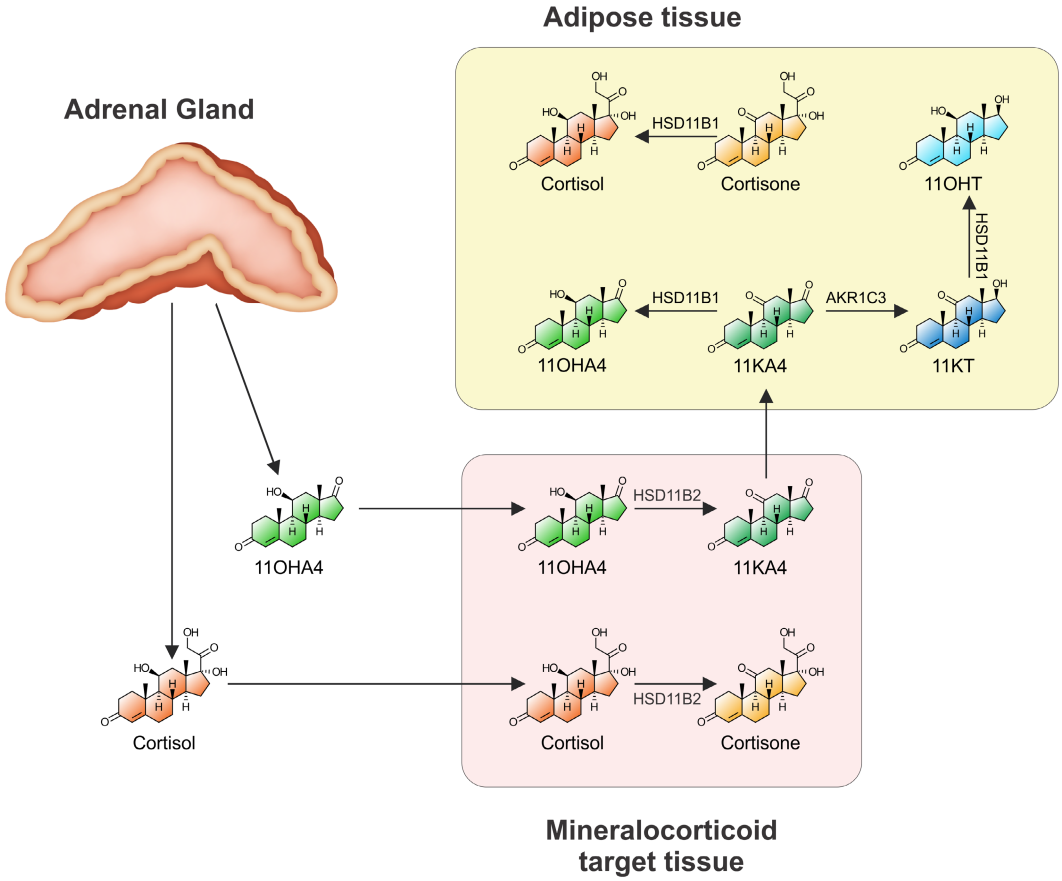

FIGURE 1 Schematic showing the peripheral metabolism of cortisol and 11OHA4. Cortisol is converted to its inactive form, cortisone, by HSD11B2 expressed in mineralocorticoid target tissues. Cortisone is in turn converted back to cortisol by HSD11B1 expressed in glucocorticoid target tissues (e.g., adipose). Like cortisol, adrenal derived 11OHA4 is a substrate for HSD11B2, yielding 11KA4. 11KA4 is a substrate for both the androgen activating enzyme AKR1C3 and HSD11B1, both of which are expressed in adipose tissue. Conversion of 11KA4 to 11OHA4 by HSD11B1 prevents the conversion of 11KA4 to the potent 11-oxygenated androgen, 11KT. The 11KT that is produced by AKR1C3 is also a substrate for HSD11B1, yielding the substantially less active androgen, 11OHT.

Here, we characterized the interplay between HSD11B1 and AKR1C3 as co-regulators of 11KT biosynthesis using a combination of in vitro, in silico, and human ex vivo and in vivo approaches including selective HSD11B1 inhibitor treatment in individuals with type 2 diabetes.

2 | MATERIALS AND METHODS

2.1 | Steroids and inhibitors

Androstenedione (4-androstene-3,17-dione), carbenoxolone ((3β,20β)-3-(3-carboxy-1-oxopropoxy)-11-oxo-olean-12-en-29-oic acid, disodium salt; CBX), cortisol (11β,17α,21-trihydroxypregn-4-ene-3,20-dione), cortisone (17α,21-dihydroxy-4-pregnene-3,11,20-trione), DHEA (5-androsten-3β-ol-17-one), DHEA sulfate (5-androsten-3β-ol-17-one-3-sulfate) and testosterone (4-androsten-17β-ol-3-one) were purchased from Sigma Aldrich. 11β-hydroxyandrostenedione (11β-hydroxy-4-androstene-3,17-dione), 11β-hydroxytestosterone (11β,17β-dihydroxyandrost-4-en-3-one), 11-ketoandrostenedione (4-androsten-3,11,17-trione) and 11-ketotestosterone (4-androsten-17β-ol-3,11-dione) were from Steraloids. The deuterated internal standards 11β-hydroxyandrostenedione-2,2,4,6,6,16,16-D7 (D7-11OHA4), 11-ketotestosterone-16,16,17-D3 (D3-11KT), androstenedione-2,2,4,6,6,16,16-D7 (D7-A4), cortisol-9,11,12,12-D4 (D4-F), DHEAS-16,16-D2 (D2-DHEAS) and testosterone-16,16,17-D3 (D3-T) were all purchased from Cambridge Isotope Laboratories. Dehydroepiandrosterone-2,2,3,4,4,6-D6 (D6-DHEA) and cortisone-2,2,4,6,6,9,12,12-D8 (D8-E) were purchased from Sigma Aldrich, while 11-ketoandostenedione-2,2,4,6,6,9,12,12,16,16-D10 (D10-11KA4) was custom-synthesized by Toronto Research Chemicals. The selective HSD11B1 inhibitor, 2-[(3S)-1-[5-(cyclohexylcarbamoyl)-6-propylsulfanylpyridin-2-yl]-3-piperidyl] acetic acid (AZD4017) was provided by AstraZeneca.

2.2 | Plasmids

The pcDNA3 vector containing AKR1C3 was provided by Prof. J. Adamski (Helmholtz Zentrum München, Germany). The pcDNA3 vectors containing HSD11B1 and hexose 6-phosphate dehydrogenase (H6PDH) were from Prof. K. Chapman (University of Edinburgh, UK). The pTAT-GRE-Elb-luc luciferase promoter reporter construct, containing two copies of the GRE was from Prof. G. Jenster (Erasmus University of Rotterdam, Netherlands), while the GR expressing plasmid (pRShGRα) was from Prof. R. Evans (Howard Hughes Medical Institute, La Jolla, USA). The pCIneo plasmid expressing the wild-type human AR was from Prof. N. Sharifi (Cleveland Clinic, Cleveland, USA). A pCIneo plasmid, containing no cDNA insert, was purchased from Promega (Wisconsin, USA).

2.3 | Cell lines

HEK293 cells were purchased from the American Type Culture Collections (ATCC) and cultured in high glucose Dulbecco's modified Eagle's medium (DMEM) supplemented with 10% FBS, 1.5 g/L $NaHCO_3$ and 1% penicillin–streptomycin and maintained at 37°C in 90% humidity and 5% CO_2. The cells were authenticated by short-tandem repeat profiling (NorthGene) and were regularly tested for mycoplasma contamination. All experiments were conducted within 20 passages from thawing a cryostock.

2.4 | Determining kinetic parameters for HSD11B1 and computational model construction

The kinetic parameters ($K_{m,app}$ and $V_{max,app}$) for HSD11B1 were determined using the methodology previously reported for AKR1C3.[16] Briefly, HEK293 cells were seeded into 10 cm^2 tissue culture dishes at a density of 2×10^5 cells per mL (10 mL per dish). After a 24 h incubation period, cells were co-transfected with 0.5 μg of HSD11B1 and 0.5 μg of H6PDH DNA using X-tremeGENE™ HP DNA transfection reagent (Roche) according to manufacturer's protocol. Following a 24 h incubation the transfected cells were re-plated into 48-well Corning® CELLBIND® plates at a density of 2×10^5 cells per mL (300 μL per well). Cells were incubated for an additional 24 h to allow for attachment before being treated with serum free media, containing appropriate steroid substrate (cortisone, 11KA4, or 11KT) at concentrations ranging from 0.1 to 10 μM. Aliquots (250 μL) for the quantification of steroid metabolism by ultra-high performance liquid chromatography tandem mass spectrometry (UHPLC–MS/MS) were collected at specific time intervals. Kinetic parameters were determined in Wolfram Mathematica (Version 13) by fitting a hyperbolic function to the data to estimate the $K_{m,app}$ and $V_{max,app}$ values by minimizing the sum of the squared differences between the experimentally determined progress curves and model, weighted by the variance using the NMinimize function. The model was fitted to triplicate data from three independent experiments. The transfection efficiency of each individual experiment was taken into account by determining the initial rate of the conversion of 100 nM 11KA4 for each independent experiment. A computational model containing the determined kinetic parameters for HSD11B1 and those previously determined for AKR1C3 was subsequently constructed. This model is comprised of ordinary differential equations (ODEs) for the metabolites, and numerical integration by making use of the NDSolve routine in Mathematica allowed for experimentally comparable metabolite profiles to be obtained. Additionally, the model was used to predict the conversion of cortisone or 11KA4 for varying HSD11B1:AKR1C3 ratios, see supplementary material for a complete model description and simulation details.

2.5 | Determining the effect of different HSD11B1:AKR1C3 ratios on cortisone and 11KA4 metabolism

HEK293 cells were seeded into 10 cm^2 tissue culture dishes at a density of 2×10^5 cells per mL (10 mL per dish). After a 24 h incubation period, dishes were co-transfected with either 0.5 μg of HSD11B1 and 0.5 μg of H6PDH or 0.5 μg of AKR1C3 and 0.5 μg of pCIneo using X-tremeGENE™ HP DNA transfection reagent (Roche). Additional dishes were transfected with 1 μg of the pCIneo (no insert) as to allow for the subsequent plating of an equal number of transfected cells at all HSD11B1:AKR1C3 ratios. After 24 h, cells were counted and combined in different ratios of HSD11B1:AKR1C3, before being re-plated into 12-well Corning® CELLBIND® surface plates at a density of 4×10^5 cells per mL (1 mL per well). After an additional incubation period of 24 h, the media was replaced with serum free DMEM containing 100 nM substrate (11KA4 or cortisone). Aliquots (500 μL) were collected 24 h after the addition of substrate for analysis by UHPLC–MS/MS, as described below.

2.6 | Determining the effect of CBX on HSD11B1 and AKR1C3 co-expression

HSD11B1 and AKR1C3 transfections were performed as described above. Transfected cells were re-plated at a

1:1 ratio of HSD11B1:AKR1C3 (2×10^5 cells/mL, 300 µL) in 48-well Corning® CELLBIND® surface plates. After 24 h, media was replaced with serum free media containing 100 nM cortisone in combination with either 10 or 100 nM 11KA4 in the absence and presence of 10 µM CBX. Aliquots (200 µL) were collected over a 24 h period for analysis by UHPLC–MS/MS. The cell viability was assessed using resazurin.

2.7 | Promoter reporter assays

To determine the effect of the HSD11B1 inhibitor CBX on AR and GR transactivation, HSD11B1 and AKR1C3 transfections were performed 24 h before co-transfections of HEK293 cells with either an AR expression plasmid (0.09 µg) and the pTAT-GRE-Elb-luc luciferase promoter reporter construct (0.9 µg) or a GR expression plasmid (0.09 µg) and the pTAT-GRE-Elb-luc luciferase promoter reporter construct (0.9 µg). HSD11B1 and AKR1C3 transfected cells were re-plated at a 1:1 ratio (4×10^5 cells/mL, 1 mL) in 12-well Corning® CELLBIND® surface plates. Following 24 h, media was replaced with serum free media containing 100 nM cortisone and 10 nM 11KA4 in the absence and presence of 10 µM CBX. At the same time the AR-GRE transfected cells and GR-GRE transfected cells were re-plated into 48-well Corning® CELLBIND® plates (3×10^5 cells/mL, 300 µL). Following a 24 h incubation with steroid, aliquots (200 µL) from the HSD11B1:AKR1C3 expressing cells were collected for the analysis of steroid metabolism by UHPLC–MS/MS. A further 300 µL conditioned media was transferred to each of the AR-GRE and GR-GRE transfected cells. These cells were incubated for a further 24 h after which cell lysates were harvested in passive lysis buffer. Reporter activity was then measured by making use of the Luciferase Assay System (Promega). The luciferase values were normalized to the protein concentration of each individual sample determined using a Thermo Scientific™ Pierce™ BCA Protein Assay kit.

2.8 | Determining the effect of ADZ4017 on 11KA4 conversion in human adipose tissue

Paired subcutaneous and omental adipose tissue was collected from eight female participants (age range 32–59 years, BMI range of 42–57 kg/m^2) undergoing elective abdominal noncancer surgery (Black Country Research Ethics Committee references 14/WM/0011 and 19/WM/0183). Written, informed consent was obtained prior to surgery and sample collection. Adipose tissue samples were transported to the laboratory at room temperature in DMEM/F12 supplemented with 33 µM biotin, 17 µM pantothenic acid and 1% penicillin–streptomycin. Connective tissue and vessels were removed and the adipose tissue washed in PBS. Tissue samples of 100–300 mg were cut and weighed. Each sample was cut into four smaller pieces for incubations with 100 nM cortisone or 100 nM 11KA4 in the presence and absence of 100 nM HSD11B1 inhibitor AZD4017 in DMEM/F12-Ham (supplemented as described above). Final solvent concentrations were adjusted to 0.003% MeOH and 0.1% DMSO in all incubations. Tissue incubations were constantly rotated in a hybrid oven at 37°C for 72 h. Medium samples were centrifuged for 10 min at 16 000 *g* and 4°C and the supernatant was used for analysis of steroid metabolism by UHPLC–MS/MS. The tissue was washed in PBS, snap frozen in liquid nitrogen and stored at −80°C for RNA extraction.

2.9 | RNA isolation and gene expression analysis from HEK293 cells

Total RNA was isolated from cells using Tri-Reagent® (Sigma) and cDNA synthesis carried out using the GoScript™ Reverse Transcription System kit (Promega). Quantitative PCR was performed using a Roche LightCycler® 96 rapid thermal cycler instrument and the KAPA SYBR® FAST qPCR Master Mix for LightCycler®. Primer sequences as follows, AKR1C3 (forward) 5′-AGCCAGGTGAGGAACTTTC-3′,[53] AKR1C3 (reverse) 5′-ATCACTGTTAAAATAGTGGAG-3′,[53] HSD11B1 (forward) 5′-CTGCCTGCTTAGGAGGTTGT-3′, HSD11B1 (reverse) 5′-CCTTGGAGCATCTCTGGTCTG-3′, the reference gene ubiquitin conjugating enzyme (UBC) (forward) 5′-CCGGGATTTGGGTCGCAG-3′, UBC (reverse) 5′-TCACGAAGATCTGCATTGTCAAG-3′. Primer efficiencies were between 90% and 110% for all primer sets. Relative gene expression was calculated using a modified form of the model described by Pfaffl.[54] Inter-experimental variations were adjusted using mean-centering.[55]

2.10 | RNA isolation and gene expression analysis from adipose tissue

Adipose tissue was homogenized in Tri-Reagent® and total RNA was isolated after phenol–chloroform extraction using the Qiagen RNeasy Mini Kit using an established protocol.[56] Reverse transcription was performed using Applied Biosystems™ TaqMan™ Reverse Transcription Reagents according to the manufacturer's protocol. qPCR was performed on an ABI 7900HT sequence detection system (Perkin Elmer, Applied Biosystems) using

TaqMan™ Gene Expression Assays (FAM-labeled) and the SensiFAST™ Probe Hi-ROX kit (Bioline). The following TaqMan™ Gene Expression Assays were used: 18S Hs99999901_s1, AKR1C3 Hs00366267_m1, HSD11B1 Hs01547870_m1.

2.11 | Determining the effect of ADZ4017 on glucocorticoid and androgen concentrations in vivo

A total of 28 participants (22 male and 6 female), all with type 2 diabetes, were recruited for a randomized, double-blind, parallel-group, placebo-controlled trial. Full ethical approval was acquired from North West Greater Manchester Central Research Ethics Committee 17/NW/0283 prior to the initiation of recruitment for the study. Informed consent was obtained from all participants after the nature and possible consequences of the study had been explained. Participants received either oral AZD4017 (400 mg) or a matched oral placebo twice daily for 35 days. Blood samples and urine were collected from individuals before first treatment and after completion of the trial and were analyzed by UHPLC–MS/MS and gas chromatography–mass spectrometry (GC–MS), respectively. Refer to Ajjan et al.[40] for further details on the study design and participants.

2.12 | Steroid extraction

Steroids were extracted from HEK293 tissue culture media using *tert*-methyl butyl ether (MTBE).[57] In brief, following the addition of an internal standard mix (100 µL containing 2 ng of D3-T and 5 ng of D7-A4, D7-11OHA4, D3-11KT and D4-F in acetonitrile) and MTBE (3:1 ratio of MTBE:media), samples were vortexed at 1500 rpm for 10 min, after which they were incubated at −80°C for 1 h, allowing for the aqueous layer to freeze. The resulting organic phase was subsequently transferred to a clean test tube and evaporated under a stream of nitrogen gas at 45°C. Extracted steroids were then reconstituted by the addition of 50% (v/v) methanol and stored at −20°C until analysis by UHPLC–MS/MS. Serum steroids and steroids in medium adipose tissue incubations were extracted using a similar method. Samples (200 µL for the serum; 500 µL for the adipose tissue conditioned medium) were mixed with 10 µL of internal standards in 50% (v/v) methanol in water (D4-F, D8-E, D6-DHEA, D7-A4, D3-T, D7-11OHA4, D10-11KA4, D3-11KT; 5 ng each for the serum, 20 ng each for adipose tissue). For serum samples, 50 µL of acetonitrile were added for protein precipitation prior to extraction and the samples vortexed. MTBE was added to each sample (1 mL for serum; 3 mL for medium from adipose tissue incubations) and the samples were vortexed at 1000 rpm for 10 min. Following incubation at room temperature for 30 min, the organic phase was transferred, dried overnight at room temperature, and reconstituted with 50% (v/v) methanol in water prior to analysis by UHPLC–MS/MS. For the measurement of serum DHEAS, 200 ng of D2-DHEAS in 20 µL of 50% methanol was added to 20 µL of serum followed by 20 µL of 1 mM $ZnSO_4$ and 100 µL of acetonitrile. The samples were centrifuged and 100 µL of the supernatant was dried and reconstituted in 50% (v/v) methanol in water prior to the UHPLC–MS/MS analysis.

2.13 | Quantification of steroids by UHPLC–MS/MS

Steroids from assays performed in HEK293 cells were separated and quantified using a UPLC high strength silica (HSS) T3 column (2.1 mm × 50 mm, 1.8 µm particle size) coupled to an ACQUITY UPLC and Xevo TQ-S triple quadrupole mass spectrometer (Waters Corporation, Milford, USA) as previously reported.[57] Steroids extracted from serum or adipose tissue incubations were separated and quantified using Phenomenex Luna Omega polar C18 column (2.1 × 50 mm, 1.6 µm particle size; Phenomenex, Macclesfield, UK) coupled to an ACQUITY UPLC and a Waters Xevo TQ-XS triple quadrupole mass spectrometer as previously described.[58] Serum DHEAS was quantified using a HSS T3 column (2.1 × 50 mm, 1.8 µm particle size; Waters) coupled to an ACQUITY UPLC and a Waters Xevo TQ-XS triple quadrupole mass spectrometer as previously described.[59,60] All steroids were quantified using Multiple Reaction Monitoring (MRM) with two transitions (quantifier and qualifier) for each. Steroids with similar MRMs were separated chromatographically.

2.14 | Quantification of urinary steroids by GC–MS

Measurement of urinary steroid metabolite excretion was carried out by a long-established GC–MS method.[61] In brief, free and conjugated steroids were extracted from 1 mL of urine by solid-phase extraction. Steroid conjugates were enzymatically hydrolyzed, re-extracted, and chemically derivatized to form methyloxime trimethyl silyl ethers. An Agilent 5975 instrument operating in selected-ion-monitoring (SIM) mode achieved sensitive and specific detection and quantification of selected steroid metabolites.

TABLE 1 Kinetic constants ($K_{m,app}$; $V_{max,app}$; V_{max}/K_m) determined for HSD11B1.

Reaction	$K_{m,app}$ (substrate) (μM)	$K_{m,app}$ (product) (μM)	$V_{max,app}$ (forward) (μM/h)[1]	$V_{max,app}$ (reverse) (1/h)[a] or (μM/h)[b]	V_{max}/K_m[2]
Cortisone → Cortisol	0.9	—	0.12	0.01[a]	0.13
11KA4 → 11OHA4	1	2.46	0.35	0.03[b]	0.35
11KT → 11OHT	0.21	—	0.05	—	0.24

[1] $V_{max,app}$ values are dependent on transfection efficiency and differ between experiments. We included the conversion of 100 nM 11KA4 to 11OHA4 in all experiments and used the initial rate to normalize the transfection efficiency, which was set to 1 for the values reported above.

[2] V_{max}/K_m values are reported for the forward reactions.

2.15 | Statistical analyses

We performed unpaired *t*-tests to compare the effect of HSD11B1 inhibition on 11-oxygenated androgen production in HEK293 cells expressing AKR1C3 and HSD11B1 and on the transactivation of the androgen receptor. Paired *t*-tests were performed to assess the effect of HSD11B1 inhibition in adipose tissue, while Wilcoxon signed-rank tests were used to assess the effect in serum and urine.

3 | RESULTS

3.1 | HSD11B1 efficiently catalyzes the 11β-reduction of 11-oxygenated androgens

Nonsteroidogenic HEK293 cells were transiently transfected to express HSD11B1 and activity assayed. Rate equations were fitted to the progress curves for three independent experiments as shown in Figure S1. A low but detectable reverse reaction rate was observed for the cortisone to cortisol and the 11KA4 to 11OHA4 reactions. Reversible kinetics were therefore used for these reactions. Our results show that the apparent K_m ($K_{m,app}$) of HSD11B1 for cortisone and 11KA4 are similar (0.9 and 1 μM), while the $K_{m,app}$ for 11KT (0.21 μM) is >4-fold lower, indicating a higher affinity towards 11KT (Table 1). However, the apparent V_{max} ($V_{max,app}$) for 11KT (0.05 μM/h) was >2-fold lower than that for cortisone (0.12 μM/h) and 7-fold lower than that for 11KA4 (0.35 μM/h). Considering the V_{max}/K_m values, an estimate of enzyme efficiency, both 11KA4 and 11KT are more efficiently converted to their respective products than the traditionally recognized HSD11B1 substrate cortisone.

3.2 | Co-expression of HSD11B1 with AKR1C3 modulates the activation of 11-oxygenated androgens

AKR1C3 is the key enzyme catalyzing the peripheral conversion of androgen precursors into active androgens.[1] We have previously shown that AKR1C3 catalyzes the conversion of 11KA4 to the potent androgen 11KT 8-fold more efficiently than the conversion of androstenedione to testosterone.[16] To determine how the co-expression of HSD11B1 with AKR1C3 would affect 11KT production, we mixed transfected HEK293 cells expressing either AKR1C3 or HSD11B1 to obtain increasing ratios of HSD11B1:AKR1C3, while keeping the number of cells expressing AKR1C3 constant. The total cell count was also kept constant by including cells transfected with an empty plasmid as required. The relative expression of HSD11B1:AKR1C3 was confirmed by qPCR (Figure 2A). Increased ratios of HSD11B1:AKR1C3 resulted in increased concentrations of cortisol being produced upon addition of 100 nM cortisone (Figure 2B), thereby confirming the increased HSD11B1 expression. Similarly, increasing the ratio of HSD11B1:AKR1C3 resulted in the concomitantly increased production of 11OHA4 from 11KA4, with 11OHA4 becoming the most abundant product when the HSD11B1:AKR1C3 ratio was increased beyond 0.1:1 (Figure 2C). Biosynthesis of 11KT was highest when AKR1C3 was expressed in the absence of HSD11B1, with increasing HSD11B1:AKR1C3 ratios resulting in a rapid decrease in the concentrations of 11KT. 11OHT initially increased as the ratio of HSD11B1:AKR1C3 increased, peaking at a ratio of 0.25:1. Further increases in the HSD11B1:AKR1C3 ratio resulted in decreased concentrations of 11OHT being produced.

Using the parameterised rate equations for HSD11B1 and those previously determined by us for AKR1C3,[16] a computational model consisting of a set of ODEs was constructed to simulate steroid metabolism in cells with both enzymes expressed:

$$\frac{d\mathrm{ka4}(t)}{dt} = -v_{\mathrm{HSD\_ka4}} - v_{\mathrm{AKR\_ka4}}; \frac{d\mathrm{oha4}(t)}{dt} = -v_{\mathrm{HSD\_ka4}}; \frac{d\mathrm{kt}(t)}{dt} = -v_{\mathrm{AKR\_ka4}} - v_{\mathrm{HSD\_kt}}; \frac{d\mathrm{oht}(t)}{dt} = -v_{\mathrm{HSD\_kt}}$$

The rate equations for HSD11B1 and AKR1C3 are given in the supplementary material. The model was able to predict the experimentally determined effect of increasing

HSD11B1:AKR1C3 ratios on the metabolism of cortisone and 11KA4, respectively (Figure 2). Note that the kinetic parameters in the mathematical model were not fitted to the experimental data for the different HSD11B1:AKR1C3 ratios, but were determined using the progress curves for the individual incubations (Figure S1). Taken together these data clearly show that HSD11B1 modulates the biosynthesis of 11KT by AKR1C3, and that the model can predict the effect of varying HSD11B1:AKR1C3 ratios.

3.3 | In vitro inhibition of HSD11B1 results in the accumulation of 11-ketotestosterone

Next, we set out to determine the effect of HSD11B1 inhibition on 11KT biosynthesis. We mixed HEK293 cells transiently transfected with either AKR1C3 or HSD11B1 at a ratio of 1:1 and simultaneously treated the cells with cortisone and 11KA4 in the absence and presence of the HSD11B1 inhibitor, carbenoxolone (CBX). We used either equimolar concentrations of cortisone and 11KA4 (100 nM each) or 10-fold excess of cortisone (100 nM) over 11KA4 (10 nM) to more closely mimic circulating concentrations.[3] Our results show that CBX reduced the production of cortisol from cortisone from 56.5 to 3.2 nM after 24 h, demonstrating effective HSD11B1 inhibition (Figure 3A,B). In the absence of CBX the majority of 11KA4 (69%) was converted to 11OHA4 by HSD11B1, with only 3.8 nM of 11KT produced from 100 nM 11KA4 by AKR1C3 (Figure 3C). However, inhibition of HSD11B1 resulted in a 7-fold increase in 11KT production after 24 h (Figure 3D). Similarly, in cells treated with 100 nM cortisone and 10 nM 11KA4, inhibition of HSD11B1 by CBX resulted in a 12-fold increase in 11KT production (0.15 nM without CBX to 1.8 nM with CBX) (Figure 3E,F). 11KT was by far the most abundant 11-oxygenated androgen following inhibition of HSD11B1. Inhibition of both the conversions from 11KA4 to 11OHA4 and 11KT to 11OHT, respectively, allowed AKR1C3 to catalyze the conversion of 11KA4 to 11KT without the need to compete for substrate and prevented the inactivation of 11KT to the less potent 11OHT. Notably, treatment with steroid substrate with or without CBX had no effect on cell viability (Figure S2). The computational model was able to independently predict the outcome of HSD11B1 inhibition under the experimental conditions (Figure 3).

3.4 | In silico analysis of the combined effect of HSD11B1:AKR1C3 co-expression and HSD11B1 inhibition on 11KT biosynthesis

After having shown that the computational model was able to individually predict both the effect of increasing HSD11B1:AKR1C3 ratios (Figure 2) and the effect of HSD11B1 inhibition (Figure 3), we used the model to simultaneously predict the effect of differing HSD11B1 and AKR1C3 expression and differing degrees of HSD11B1 inhibition on the conversion of 10 nM 11KA4 to 11OHA4,

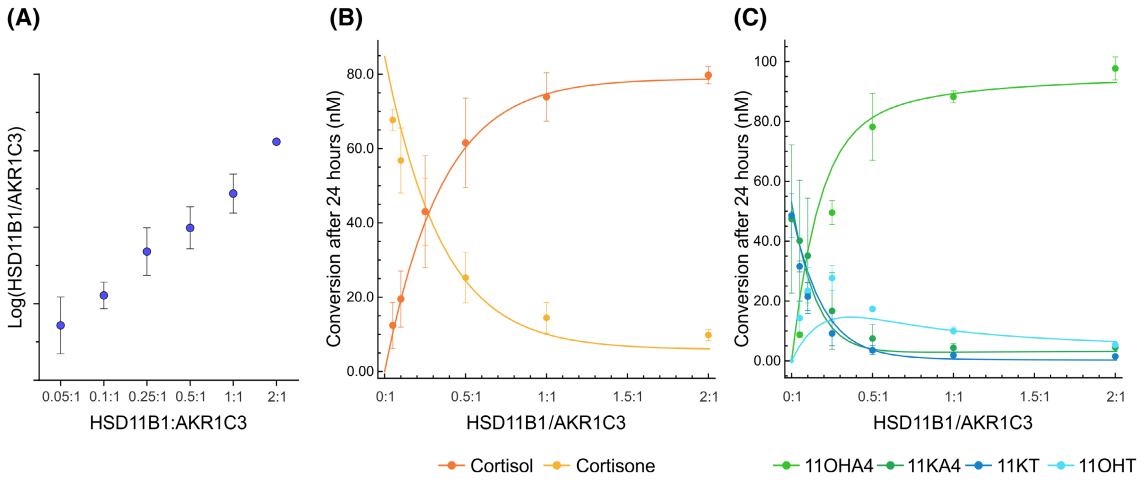

FIGURE 2 Increased HSD11B1:AKR1C3 ratios modulate the biosynthesis of 11KT. (A) qPCR data confirming the increase in HSD11B1 expression relative to that of AKR1C3 at the different HSD11B1:AKR1C3 ratios. (B) The conversion of cortisone (0.1 μM) to cortisol by increasing the ratios of HSD11B1:AKR1C3 after 24 h (C). The conversion of 11KA4 (0.1 μM) to 11OHA4, 11KT and 11OHT by increasing the ratios of HSD11B1:AKR1C3 after 24 h. For (B) and (C) the experimental data from the ratio experiments are shown as points with error bars, while the computational models' predictions are shown with the solid connecting lines. All results are shown as mean ± SEM of three independent experiments.

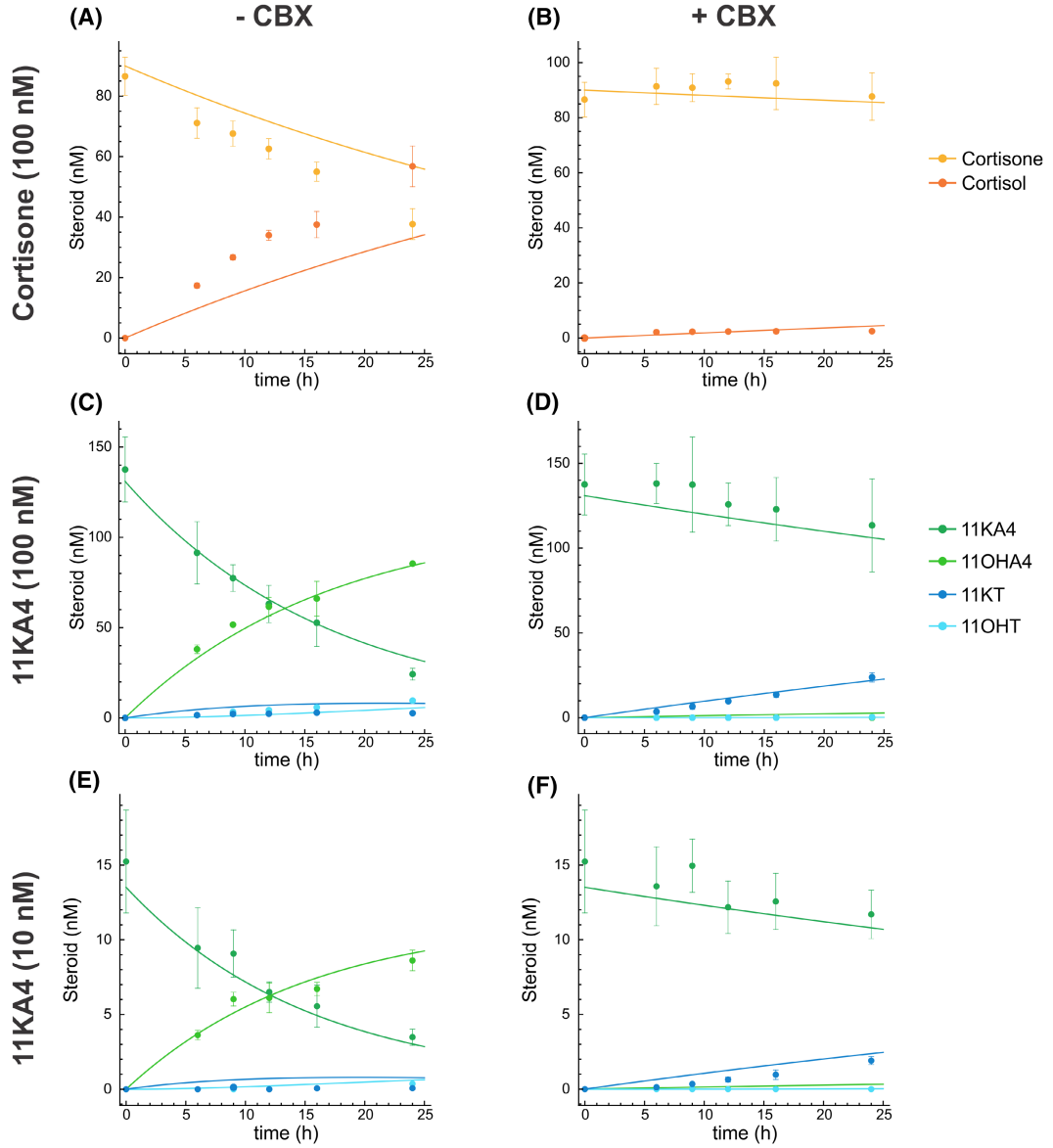

FIGURE 3 Inhibition of HSD11B1 by carbenoxolone (CBX) inhibits the biosynthesis of cortisol, but allows for the increased AKR1C3-mediated production of 11KT when HSD11B1 and AKR1C3 are co-expressed. HEK293 cells expressing HSD11B1 and AKR1C3 were combined at a ratio of 1:1 and treated with either 100 nM cortisone (A and B) and 100 nM 11KA4 (C and D) with and without CBX (10 μM) or 100 nM cortisone and 10 nM 11KA4 (E and F) with or without CBX (10 μM). The experimental data from the time course experiment is shown as points with error bars, while the computational models' predictions are shown with the solid lines. All results are shown as mean ± *SD* of a single biological experiment performed in triplicate. This enabled the model to predict the outcomes from one experiment with the same transfection efficiency.

11KT and 11OHT after 24 h (Figure 4). These results confirmed that HSD11B1 strongly modulates the biosynthesis of 11KT by competing for the precursor, 11KA4, and by converting the 11KT that is formed to the less potent androgen 11OHT. The inhibition of HSD11B1 reduced these effects under all HSD11B1:AKR1C3 ratios tested leading to increased production of 11KT. Notably, lower ratios of HSD11B1:AKR1C3 were more sensitive to HSD11B1 inhibition, more quickly leading to increased 11KT concentrations as the level of inhibition was increased. Higher absolute concentrations of 11KT were also produced by lower ratios of HSD11B1:AKR1C3 (AKR1C3 was kept constant) when HSD11B1 was inhibited up to the maximum simulated I/K_i value of 10. Near complete inhibition of HSD11B1 ($I/K_i = 100$), however, negated the effect of the HSD11B1:AKR1C3 ratio with 11KT production dependent only on AKR1C3 (Figure S3). The effect of HSD11B1 inhibition is therefore dependent on the degree of inhibition, the ratio of HSD11B1:AKR1C3 and the absolute expression level of HSD11B1 and AKR1C3.

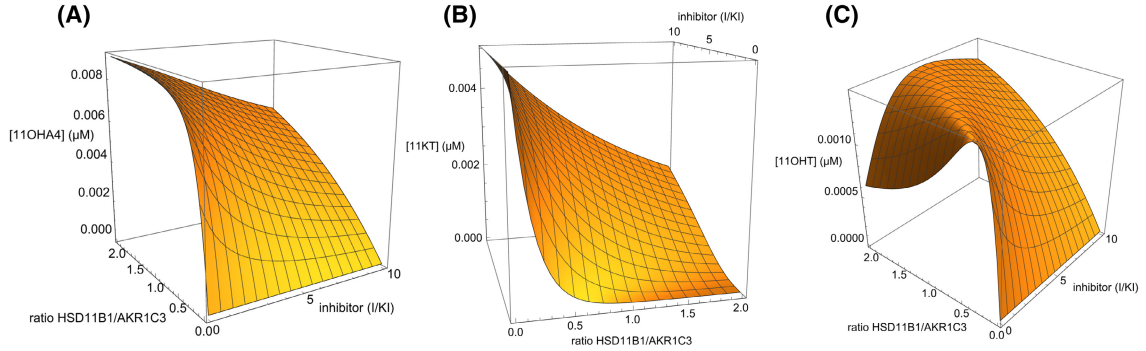

FIGURE 4 Computational model of the effect of varying HSD11B1:AKR1C3 ratios and different levels of HSD11B1 inhibition on the resulting concentrations of 11OHA4 (A), 11KT (B) and 11OHT (C). The model varies the ratio of HSD11B1:AKR1C3 as in Figure 2 and estimates the effect of different levels of HSD11B1 inhibition on the conversion of 10 nM 11KA4 after 24 h as in Figures 2 and 3.

3.5 | Selective HSD11B1 inhibition increases AR activation in vitro

To investigate the potential biological impact of HSD11B1 inhibition, we combined HEK293 cells expressing AKR1C3 or HSD11B1 at a 1:1 ratio and incubated the cells with 100 nM cortisone and 10 nM 11KA4 in the absence and presence of CBX for 24 h. The conditioned media were then transferred to HEK293 cells transiently transfected with either a plasmid expressing the glucocorticoid receptor (GR) or the androgen receptor (AR), and a luciferase reporter construct. The GR- and AR-mediated induction of luciferase was subsequently measured after an additional 24 h incubation. As expected, HSD11B1 mediated the conversion of cortisone to cortisol, with the resulting cortisol increasing the transactivation of the GR (94-fold induction). Inhibition of HSD11B1 with CBX reduced cortisol production 32-fold (Figure 5A) and resulted in a 34-fold decrease in GR transactivation (Figure 5B). Conversely, inhibition of HSD11B1 resulted in a 7-fold increase in transactivation of the AR due to significantly increased 11KT biosynthesis (Figure 5C,D). Basal levels of AR transactivation in the absence of CBX and 11KT were due to the presence of low concentrations of 11OHT (0.81 nM; Figure S4), which is a partial agonist of the AR.[11,62] It should be noted that we observed that CBX weakly antagonizes the AR (Figure S5), hence, the induction of the AR was likely underestimated. Nonetheless, taken together, these data demonstrate that while inhibition of HSD11B1 results in the desired decrease in GR transactivation, this is accompanied by a shift towards AR transactivation.

3.6 | Selective HSD11B1 inhibition increases 11KT production in female human adipose tissue ex vivo

We next set out to determine the effect of HSD11B1 inhibition on 11KT biosynthesis in paired subcutaneous and omental adipose tissue samples from women undergoing elective bariatric surgery. For these experiments we employed the selective HSD11B1 inhibitor AZD4017.[63] The conversion of cortisone to cortisol was reduced to 3% of the uninhibited conversion rate in subcutaneous adipose tissue treated with AZD4017, thereby confirming effective HSD11B1 inhibition (Figure 6A). Following incubation of subcutaneous adipose tissue with 11KA4 (100 nM), the most abundant product formed in the absence of AZD4017 was 11OHT (60.1% of total products formed), followed by 11OHA4 (23.4%) and 11KT (16.5%) (Figure 6F). The biosynthesis of both 11KT and 11OHT is dependent on AKR1C3 activity and the observed sum of 11KT and 11OHT (76.6% of products formed) suggested substantial AKR1C3 expression. This was confirmed by qPCR analysis, which showed higher AKR1C3 expression relative to that of HSD11B1 (Figure 6C). However, HSD11B1 converted 78.5% of the 11KT formed to the less active 11OHT. Inhibition of HSD11B1 by AZD4017, resulted in a 5-fold increase in 11KT, with 11KT becoming the most abundant product (85.6%) (Figure 6G). This was accompanied by significant decreases in the production of both 11OHA4 and 11OHT (21-fold and 4.5-fold, respectively).

Marginally lower conversion of cortisone to cortisol was observed in omental adipose tissue as compared to subcutaneous tissue, with AZD4017 again effectively inhibiting HSD11B1 activity (Figure 6B). Treatment with AZD4017 again resulted in a significant decrease in 11OHA4 and 11OHT concentrations, with an accompanying 4-fold increase in 11KT production (Figure 6H,I).

The sum of 11KT and 11OHT (66.0%) was lower in the omental tissue than in subcutaneous tissue (76.6%) illustrating lower AKR1C3 expression as confirmed by qPCR (Figure 6C,D). The ratio of HSD11B1 over AKR1C3 expression was lower in subcutaneous than omental adipose tissue (Figure 6E), favoring androgen activation in subcutaneous tissue vs glucocorticoid activation in omental tissue. The metabolism of 11KA4 and the effect of AZD4017 inhibition in human adipose tissue was simulated with

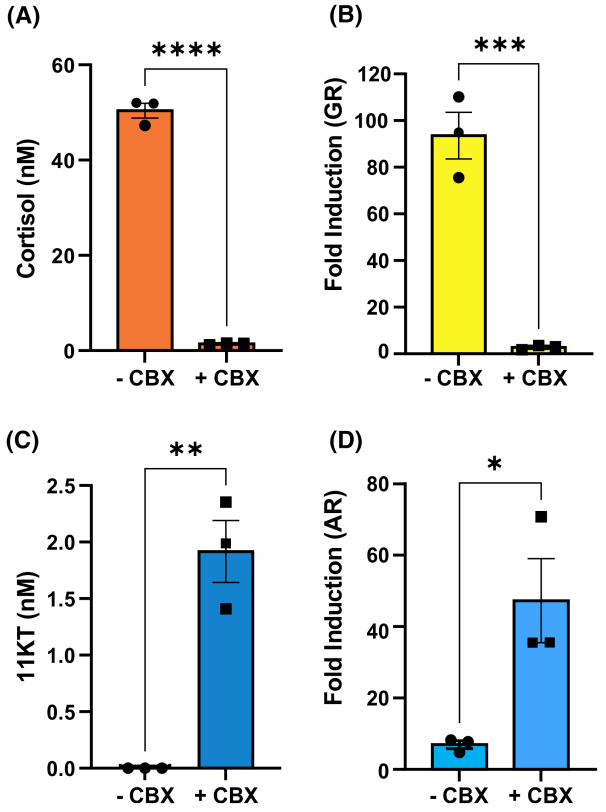

FIGURE 5 Inhibition of HSD11B1 by carbenoxolone (CBX) results in decreased cortisol production (A) and an accompanying decrease in transactivation of the glucocorticoid receptor (B), but increased production of 11KT (C) and transactivation of the androgen receptor (D). HEK293 cells expressing HSD11B1 and AKR1C3 were combined at a ratio of 1:1 and treated with 100 nM cortisone and 10 nM 11KA4 with or without CBX (10 μM). After 24 h the conditioned media was transferred to HEK293 cells transiently transfected with either a plasmid expressing the glucocorticoid receptor (GR) and a luciferase reporter construct or a plasmid expressing the androgen receptor (AR) and the same luciferase reporter construct. Luciferase was assayed after an additional 24 h incubation and is shown as the fold-induction relative to a vehicle control. All results are shown as means ± SEM of three biological experiments. *p*-values were calculated using unpaired *t*-tests (*$p < .05$; **$p < .01$; ***$p < .001$; and ****$p < .0001$).

the mathematical model that was constructed using conversion data obtained from transfected HEK293 cells. The expression levels of HSD11B1 and AKR1C3 in the adipose tissue relative to that in transfected HEK293 cells therefore needed to be estimated. This was achieved by fitting the expression levels of HSD11B1 to the cortisone to cortisol conversion data (Figure 6A,B) and then using an AKR1C3 activity based on the AKR1C3/HSD11B1 expression ratio as determined by qPCR (Figure 6C,D). This allowed the model to predict the conversion of 11KA4 to the respective products over time. These simulations revealed the initial accumulation of 11KT, prior to the time dependent conversion of this product to 11OHT by HSD11B1 (Figure 6F,H). Inhibition of HSD11B1 eliminated the latter conversion yielding only 11KT and illustrated that the amount of 11KT formed over time was dependent on the absolute expression levels of AKR1C3.

Taken together, these data indicate that inhibition of HSD11B1 in adipose tissue leads to a shift in the metabolism of 11-oxygenated androgens resulting in increased 11KT biosynthesis.

3.7 | In vivo treatment with a selective HSD11B1 inhibitor increases circulating 11KT concentrations

After having shown that inhibition of HSD11B1 in adipose tissue shifts the metabolism of 11-oxygenated androgens towards 11KT biosynthesis, we next set out to determine if inhibition of HSD11B1 would alter circulating concentrations of 11KT. We therefore measured a panel of 11-oxygenated androgens as well as cortisol and cortisone in the serum of individuals with type 2 diabetes who had received treatment with the selective HSD11B1 inhibitor AZD4017 during a randomized, double-blind, parallel-group, placebo-controlled phase 2b pilot trial.[40] Paired (day 0 and day 35) samples were available for 18 participants (13 men and 5 women; median BMI 32.2 kg/m^2 range 25.0–47.5 kg/m^2; median age 64.5, range 28–84 years), with 11 randomized to HSD11B1 inhibitor treatment (7 men and 4 women) and 7 (6 men and 1 woman) to placebo.

Our measurements confirmed that AZD4017 significantly reduced the serum cortisol/cortisone ratio, indicating effective HSD11B1 inhibition as previously reported for selected urinary glucocorticoid metabolites by LC–MS/MS,[40] and further confirmed here by GC–MS (Figure S6). However, concomitantly, circulating 11KT concentrations significantly increased 2.5-fold (from 1.7 to 4.3 nM) following treatment with 400 mg AZD4017 twice daily for 35 days. This was accompanied by a significant, 2-fold decrease in 11OHT concentrations and a 4-fold decrease in the 11OHT/11KT ratio (Figure 7). While the circulating concentrations of the 11-oxygenated androgen precursors 11OHA4 and 11KA4 did not change, a small, but significant decrease was also observed for the 11OHA4/11KA4 ratio. These changes were also reflected by a significant increase in the urinary metabolite 11-oxoandrosterone, which is derived from 11KA4 and 11KT,[64] and a 6-fold decrease in the 11β-hydroxyandrosterone/11-oxoandrosterone ratio (Figure 7). No changes in the serum concentrations of 11-oxygenated androgens were observed in the placebo-treated group (Figure S7).

When considering correlations between the changes in circulating steroid concentrations, it is interesting to note

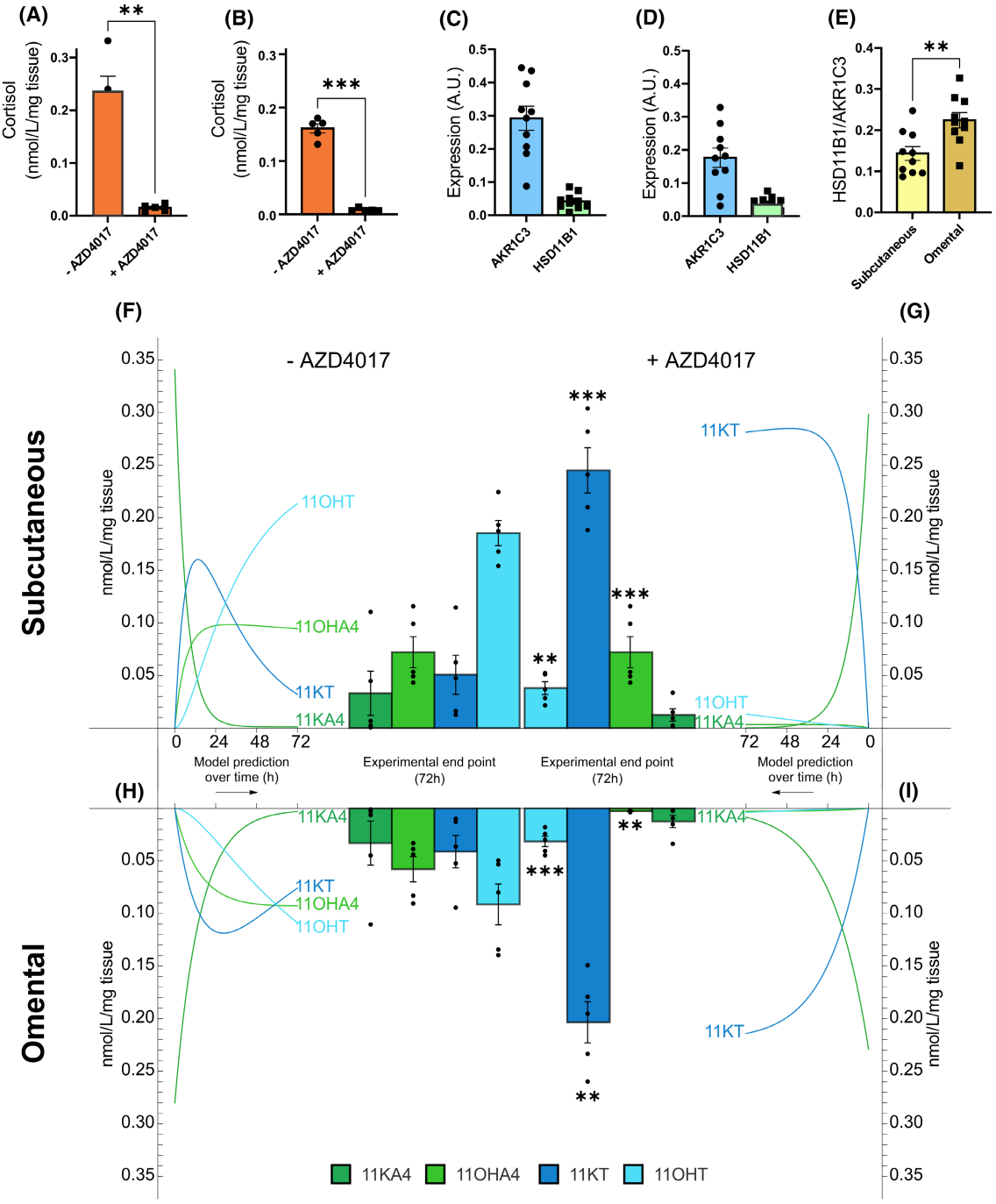

FIGURE 6 Inhibition of HSD11B1 by AZD4017 in human subcutaneous (A, F, G) and omental (B, H, I) adipose tissue results in the increased production of 11KT. Adipose tissue was incubated ex vivo with 100 nM cortisone (A, B) or 11KA4 (F–I) with or without AZD4017 (100 nM) for 72 h. The mathematical model's prediction of the conversion over time is shown next to the experimentally determined end point data after the 72 h incubation. Expression of AKR1C3 and HSD11B1 in subcutaneous (C) and omental (D) adipose tissue was measured by qPCR. The expression ratio of HSD11B1:AKR1C3 were determined for both adipose tissue subtypes (E). *p*-values were calculated using Wilcoxon signed-rank tests (*$p < .05$; **$p < .01$; and ***$p < .001$).

that the cortisol/cortisone ratio is highly correlated with the change in both the ratios of 11OHA4/11KA4 ($R = .893$; $p < .001$) and 11OHT/11KT ($R = .686$; $p < .01$), but not with the change in circulating 11KT ($R = -.375$; $p = .126$) (Table S1).

4 | DISCUSSION

The relatively recent identification of 11-oxygenated androgens as important contributors to the human androgen pool has prompted a re-evaluation of existing

paradigms. One such paradigm is the idea that the two HSD11B isoforms are predominantly involved in the peripheral metabolism of glucocorticoids. We and others have previously shown that HSD11B1 and HSD11B2 are essential for the interconversion of the 11β-hydroxyl and 11-keto forms of the 11-oxygenated androgens.[11,20] We have also previously shown that 11KA4, but not 11OHA4, is a substrate for the key androgen-activating enzyme AKR1C3.[16,17] Therefore, HSD11B2 plays a vital role in catalyzing the conversion of adrenal-derived 11OHA4 to 11KA4, which can then be converted to the potent androgen 11KT by AKR1C3.[13] One of the main sites of AKR1C3 expression and peripheral androgen activation is adipose tissue[14,15] which also abundantly expresses HSD11B1.[18,19,22] Paulukinas et al. have previously observed that co-expression of HSD11B1 with AKR1C3 in differentiated SGBS adipocyte cells may prevent the accumulation of 11KT, thus suggesting that HSD11B1 may protect from androgen excess.[17] Here, using a combination of in vitro, in silico and ex vivo studies, we demonstrate that co-expression of HSD11B1 with AKR1C3 modulates peripheral biosynthesis of 11KT, first, by competing with AKR1C3 for the substrate 11KA4, and, second, by converting much of the resulting 11KT to the less potent androgen 11OHT. We demonstrated that inhibition of HSD11B1 results in significantly increased 11KT biosynthesis as shown by us in vitro, in silico, ex vivo and in a phase 2a study comparing the effects of 35 days of treatment with the selective HSD11B1 inhibitor AZD4017 to placebo treatment. Our data show that HSD11B1 inhibition does not only alter local, adipose tissue-specific 11KT concentrations, but also systemic levels, thus emphasizing that peripheral tissues expressing AKR1C3 are essential for

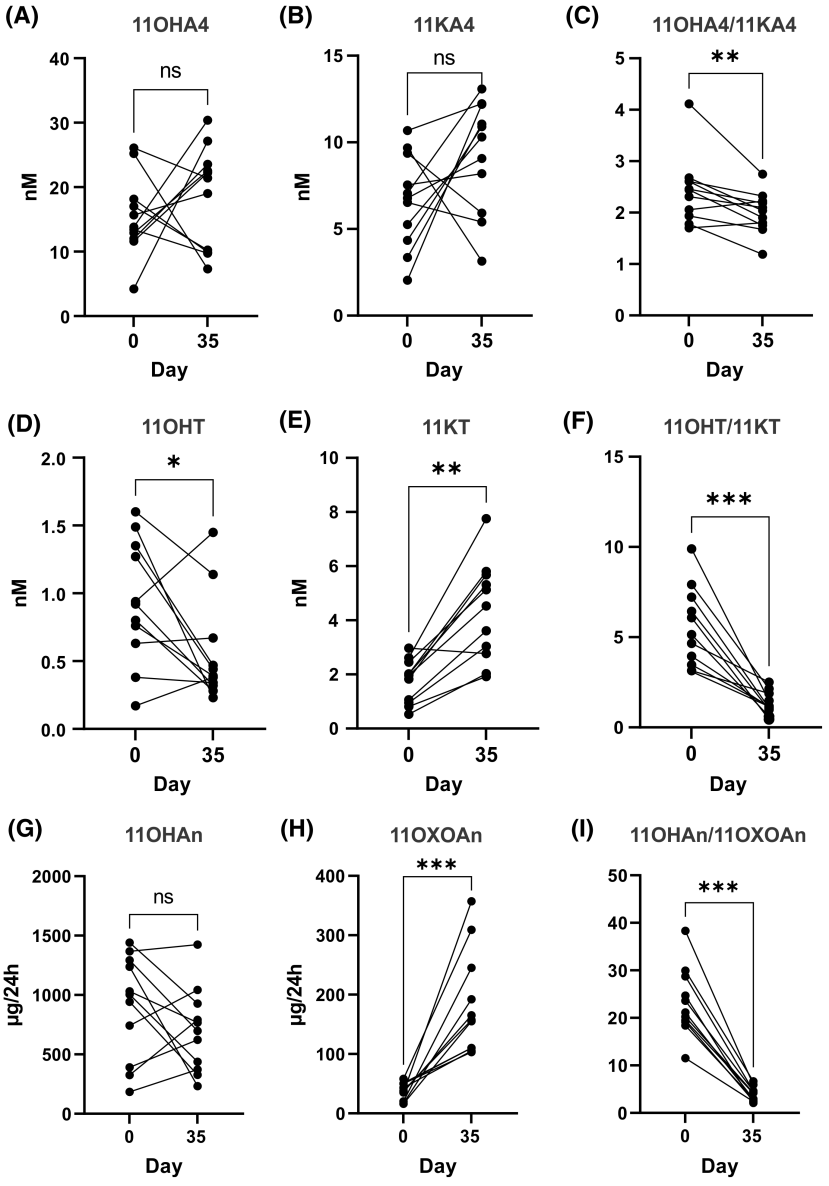

FIGURE 7 Inhibition of HSD11B1 by oral administration of AZD4017 (400 mg twice daily) for 35 days ($n = 11$) changes the serum (A–F) and urinary (G–I) profile of 11-oxygenated androgens and their metabolites, with significant increases in the circulating concentration of the potent androgen 11KT. *p*-values were calculated using Wilcoxon signed-rank tests (*$p < .05$; **$p < .01$; and ***$p < .001$). Serum concentrations of classic androgens are shown in Figure S8.

11KT biosynthesis.[13] Collectively, our findings show that under normal circumstances HSD11B1 plays an important novel role in preventing 11KT accumulation, in addition to its well-known role in local glucocorticoid activation.

Our findings are of immediate clinical relevance, particularly in women, where circulating concentrations of 11KT are similar to testosterone concentrations.[3,6,7,65] Therefore, increasing 11KT due to HSD11B1 inhibition markedly increases the total circulating pool of active androgens in women. This increase in androgen load is significant given that 11KT has shown functional activity comparable to testosterone[5,62,66] and increased circulating androgens have been linked to a significantly greater risk of type 2 diabetes in women.[43] Moreover, there is growing evidence that androgens drive the risk of common metabolic disorders, including type 2 diabetes, hypertension, cardiovascular disease and MASLD,[15,43–52,67–69] in women with PCOS where androgen excess is a hallmark.[69] Notably, O'Reilly et al. have previously shown that local AKR1C3-mediated androgen activation in adipose tissue drives lipotoxicity in women with PCOS.[15] They propose a vicious cycle in which increased androgen generation in adipose tissue results in lipid accumulation, increased fat mass and as a result systemic insulin resistance. This cycle is completed by the insulin-induced stimulation of AKR1C3 expression in adipose, leading to increased androgen activation. Given that 11KA4 is the preferred substrate for AKR1C3, increased insulin-induced AKR1C3 expression would therefore lead to significantly more 11KT being produced, which would be further increased by HSD11B1 inhibition.[16,17,70]

Our finding of increased 11KT biosynthesis to clinically highly relevant concentrations occurring after HSD11B1 inhibition therefore needs to be taken into account when considering HSD11B1 inhibition as treatment for type 2 diabetes or metabolic syndrome in women, as the beneficial effects of reduced local glucocorticoid activation could be offset by opposing metabolic effects due to increased 11KT concentrations and AR signaling. This is highly relevant for the recently proposed use of HSD11B1 inhibitors in ameliorating the metabolically adverse consequences of mild autonomous cortisol excess (MACS) due to adrenal adenomas[71] as affected patients are predominantly female.[72]

Notably, quantification of AKR1C3 and HSD11B1 expression levels in subcutaneous and omental adipose tissue revealed a degree of interpersonal variation. Our computational simulations revealed that variations in the relative, as well as the absolute expression levels of HSD11B1 and AKR1C3 would result in individual differences in the amount of 11KT produced as well as the magnitude of change upon HSD11B1 inhibition. Indeed, this biological variation was reflected in both the ex vivo adipose tissue conversion data and the serum concentrations of 11KT before and after administration of AZD4017 in individuals with type 2 diabetes. Our simulations suggest that when considering 11KT biosynthesis, individuals with higher HSD11B1 expression relative to AKR1C3 would be less responsive to partial HSD11B1 inhibition. However, if HSD11B1 activity is completely abolished by inhibition then the amount of 11KT produced is dependent of the absolute levels of AKR1C3 expressed. Increased 11KT concentrations are therefore not solely dependent on the inhibition of HSD11B1, but also on the amount of AKR1C3 expressed. Notably, AKR1C3 expression correlates with BMI in subcutaneous, but not omental, adipose tissue and its expression is upregulated by insulin.[14,15,17] Women with insulin resistance and obesity due to metabolic syndrome are therefore likely to have high expression levels of AKR1C3,[14,15] which would result in greater increases in 11KT upon inhibition of HSD11B1. Thus, while such women may benefit from the local reduction of glucocorticoid activation by HSD11B1 inhibition in adipose tissue, they may be primed to generate more 11KT. Indeed, we noted that the expression of AKR1C3 was higher than that of HSD11B1 in adipose tissue obtained from women with obesity undergoing elective bariatric surgery. As a result, the conversion of 11KA4 yielded more 11KT and 11OHT combined (both requiring AKR1C3 activity) than 11OHA4. In subcutaneous adipose tissue, which had a lower HSD11B1:AKR1C3 ratio compared to omental adipose tissue, 11OHT was the most abundant product, demonstrating effective conversion of 11KA4 to 11KT by AKR1C3 and subsequent conversion of 11KT to 11OHT by HSD11B1. Similarly, we noted that in our clinical cohort, which consisted of individuals with type 2 diabetes (BMI mostly in the obese range), the mean circulating 11OHT concentration was ≥2-fold higher than previously reported for healthy individuals thus suggesting high peripheral AKR1C3 expression.[3] Interestingly, a previous ex vivo study found that androgen exposure upregulates HSD11B1 expression in adipose tissue[73] emphasizing that inactivation of 11-oxygenated androgens by HSD11B1 might be a protective mechanism, that no longer suffices once AKR1C3 is significantly upregulated, e.g., in the context of PCOS.[15]

Increased 11KT concentrations following HSD11B1 inhibition are unlikely to be a concern in men as the metabolic effects of androgens are sexually dimorphic. In men, reduced androgen concentrations are associated with adverse metabolic consequences, including insulin resistance, type 2 diabetes and metabolic syndrome, and as such increased 11KT levels have the potential to be beneficial.[43,68,74] Glucocorticoids are, however, also known to have sexually dimorphic effects, which are further complicated by the crosstalk between glucocorticoids and androgens.[75–77] Unfortunately, the vast majority of HSD11B1 inhibitor clinical studies did not report sex-specific outcomes for HSD11B1 inhibition.[34–38] Larger sex-specific

studies are therefore needed to fully assess the benefits of HSD11B1 inhibition in relation to metabolic conditions, while taking into account potential opposing androgenic effects in women, resulting from increased 11KT.

One recent study by Hardy et al. investigated the effects of HSD11B1 inhibition in women with obesity and Idiopathic Intracranial Hypertension.[41] Twice daily administration of 400 mg AZD4017 for 12 weeks had no effect on fasting glucose, fasting insulin, insulin resistance or HbA1c, in agreement with our hypothesis that androgenic effects may counter beneficial metabolic effects of reduced glucocorticoid concentrations. Furthermore, this study found no effect of HSD11B1 inhibition on adipose or bone composition, but did report reduced cholesterol and increased HDL with HSD11B1 inhibition suggesting that women do exhibit some cardioprotective responses to HSD11B1 inhibition. Importantly, Hardy et al. also reported increased lean muscle mass with HSD11B1 inhibition, which correlated with increased testosterone and 11-oxygenated androgen precursor (11OHA4 and 11KA4) levels; however, they did not report 11KT concentrations.

Increased adrenal output of 11OHA4 is not unexpected with HSD11B1 inhibition, which leads to reduced negative feedback on the HPA-axis, increased ACTH levels and increased adrenal output of cortisol and adrenal androgen precursors.[41] While we did not observe increased serum 11OHA4 concentrations in the current study, we cannot exclude that increased adrenal output of this precursor contributed to the observed increase in 11KT biosynthesis. In fact, this is likely the case as circulating 11OHA4 concentrations were not reduced despite inhibition of HSD11B1 and the resulting significant decrease in the 11OHA4/11KA4 ratio. Furthermore, the original clinical trial observed a significant increase in serum DHEAS, a marker of adrenal C19 steroid biosynthesis, thus confirming the stimulation of adrenal steroidogenesis.[40] Despite the potential increase in adrenal 11OHA4 biosynthesis, our in vitro, ex vivo and in silico data unequivocally show that HSD11B1 modulates the peripheral biosynthesis of 11KT and that inhibition of HSD11B1 results in increased peripheral 11KT production irrespective of adrenal 11OHA4 output.

This study highlights that HSD11B1 inhibition may not be as effective as previously anticipated for the treatment of metabolic conditions in women due to the concomitant increase in the active androgen pool. However, the current data does not call into question the safety or efficacy of HSD11B1 inhibitors such as AZD4017, which has been shown to be well tolerated,[39–41,63,78] but rather highlights that the condition targeted by the use of HSD11B1 inhibitors needs to be carefully considered. To date, AZD4017 has shown promise in the treatment of Idiopathic Intracranial Hypertension and wound healing in adults with type 2 diabetes, thus warranting further studies.[40,41] It may also be interesting to consider HSD11B1 inhibition in oophorectomized women. In this setting, the increased biosynthesis of 11KT due to HSD11B1 inhibition may be beneficial in offsetting the androgen deficiency due to oophorectomy, while reduced local glucocorticoid activation has the potential to protect against glucocorticoid induced osteoporosis, especially against the backdrop of reduced estrogen biosynthesis.[79–81]

While the current study focusses on the regulation of 11KT biosynthesis by HSD11B1 in adipose tissue, HSD11B1 is also abundantly expressed in liver and as such the hepatic conversion of 11KA4 to 11OHA4 and 11KT to 11OHT may also regulate systemic 11KT levels, with inhibition of hepatic HSD11B1 by AZD4017 contributing to the observed increase in 11KT levels.[18,19]

In summary, our findings indicate that HSD11B1 plays an essential role in modulating the amount of 11KT produced by AKR1C3 expressed in adipose tissue. As a result, inhibition of HSD11B1 does not just reduce local glucocorticoid activation, but also alters the biosynthesis of the potent 11-oxygenated androgen 11KT. In women, the significant increase in 11KT concentrations may have metabolically opposing effects that attenuate the beneficial reduction of glucocorticoid activation in metabolic tissue. It is therefore imperative that future HSD11B1 inhibitor studies consider both the glucocorticoid and androgen pools and that sex-specific effects are systematically investigated.

AUTHOR CONTRIBUTIONS

Karl-Heinz Storbeck, Wiebke Arlt, and Lina Schiffer were responsible for study concept and design. Lina Schiffer and Imken Oestlund conducted the experiments. Jacky L. Snoep performed all computational modeling. Lina Schiffer, Imken Oestlund, Jacky L. Snoep, Lorna C. Gilligan, Angela E. Taylor, and Karl-Heinz Storbeck analyzed the data. Alexandra J. Sinclair and Rishi Singhal provided human adipose tissue. Ana Tiganescu, Ramzi Ajjan, and Adrian Freeman provided the serum and urine from a phase 2b pilot trial with AZD4017. Angela E. Taylor and Lorna C. Gilligan conducted the analysis of clinical samples by LC–MS/MS and GC–MS, respectively. Karl-Heinz Storbeck, Lina Schiffer, and Imken Oestlund drafted the manuscript. Wiebke Arlt, Ana Tiganescu, and Jacky L. Snoep critically reviewed the manuscript. All authors reviewed and approved the final version of the manuscript. Karl-Heinz Storbeck and Wiebke Arlt obtained funding. Lina Schiffer and Imken Oestlund contributed equally to this work. Lina Schiffer was selected as the first of the two authors as she was involved in the conceptualization of the study.

ACKNOWLEDGEMENTS

This work has been supported by the National Research Foundation of South Africa (Grant Numbers 132503

and SRUG2204052159 to KHS); the Academy of Medical Sciences UK (Newton Advanced Fellowship NAF004\1002 to KHS); the Wellcome Trust (Investigator Grant WT209492/Z/17/Z to WA); a Medical Research Council Confidence in Concept Award to AT (MC_PC_15046); and a SARChI DST/NRF grant (82813 to JS).

DISCLOSURES

The authors declare no conflicts of interest.

DATA AVAILABILITY STATEMENT

The data that support the findings of this study are available in the results and/or supplementary material of this article. The computational model and simulated data are available at https://fairdomhub.org/investigations/658, and can be cited via DOI: https://doi.org/10.15490/fairdomhub.1.investigation.658.1.

ORCID

Lina Schiffer https://orcid.org/0000-0001-8540-4861
Imken Oestlund https://orcid.org/0009-0005-4621-7541
Jacky L. Snoep https://orcid.org/0000-0002-0405-8854
Lorna C. Gilligan https://orcid.org/0000-0002-0708-2999
Angela E. Taylor https://orcid.org/0000-0002-5835-5643
Alexandra J. Sinclair https://orcid.org/0000-0003-2777-5132
Rishi Singhal https://orcid.org/0000-0002-2797-2569
Adrian Freeman https://orcid.org/0009-0007-0413-5657
Ramzi Ajjan https://orcid.org/0000-0002-1636-3725
Ana Tiganescu https://orcid.org/0000-0003-3688-2204
Wiebke Arlt https://orcid.org/0000-0001-5106-9719
Karl-Heinz Storbeck https://orcid.org/0000-0003-1669-6383

REFERENCES

1. Pretorius E, Arlt W, Storbeck K-H. A new dawn for androgens: novel lessons from 11-oxygenated C19 steroids. *Mol Cell Endocrinol*. 2017;441:76-85.
2. Turcu AF, Rege J, Auchus RJ, Rainey WE. 11-Oxygenated androgens in health and disease. *Nat Rev Endocrinol*. 2020;16:284-296.
3. Schiffer L, Kempegowda P, Sitch AJ, et al. Classic and 11-oxygenated androgens in serum and saliva across adulthood: a cross-sectional study analyzing the impact of age, body mass index, and diurnal and menstrual cycle variation. *Eur J Endocrinol*. 2023;188:1-15.
4. Storbeck K-H, O'Reilly MW. The clinical and biochemical significance of 11-oxygenated androgens in human health and disease. *Eur J Endocrinol*. 2023;188:R98-R109.
5. Pretorius E, Africander DJ, Vlok M, Perkins MS, Quanson JL, Storbeck K-H. 11-ketotestosterone and 11-ketodihydrotestosterone in castration resistant prostate cancer: potent androgens which can no longer be ignored. *PLoS One*. 2016;11:e0159867.
6. Nanba AT, Rege J, Ren J, Auchus RJ, Rainey WE, Turcu AF. 11-Oxygenated C19 steroids do not decline with age in women. *J Clin Endocrinol Metab*. 2019;104:2615-2622.
7. Skiba MA, Bell RJ, Islam RM, Handelsman DJ, Desai R, Davis SR. Androgens during the reproductive years: what is normal for women? *J Clin Endocrinol Metab*. 2019;104:5382-5392.
8. O'Reilly MW, Kempegowda P, Jenkinson C, et al. 11-oxygenated C19 steroids are the predominant androgens in polycystic ovary syndrome. *J Clin Endocrinol Metab*. 2017;102:840-848.
9. Turcu AF, Nanba AT, Chomic R, et al. Adrenal-derived 11-oxygenated 19-carbon steroids are the dominant androgens in classic 21-hydroxylase deficiency. *Eur J Endocrinol*. 2016;174:601-609.
10. Nowotny HF, Braun L, Vogel F, et al. 11-Oxygenated C19 steroids are the predominant androgens responsible for hyperandrogenemia in Cushing's disease. *Eur J Endocrinol*. 2022;187:663-673.
11. Storbeck K-H, Bloem LM, Africander DJ, Schloms L, Swart P, Swart AC. 11β-hydroxydihydrotestosterone and 11-ketodihydrotestosterone, novel C19 steroids with androgenic activity: a putative role in castration resistant prostate cancer? *Mol Cell Endocrinol*. 2013;377:135-146.
12. Snaterse G, van Dessel LF, van Riet J, et al. 11-Ketotestosterone is the predominant active androgen in prostate cancer patients after castration. *JCI Insight*. 2021;6:e148507.
13. Storbeck K-H. A commentary on the origins of 11-ketotestosterone. *Eur J Endocrinol*. 2022;187:C5-C8.
14. Quinkler M, Sinha B, Tomlinson JW, Bujalska IJ, Stewart PM, Arlt W. Androgen generation in adipose tissue in women with simple obesity—a site-specific role for 17β-hydroxysteroid dehydrogenase type 5. *J Endocrinol*. 2004;183:331-342.
15. O'Reilly MW, Kempegowda P, Walsh M, et al. AKR1C3-mediated adipose androgen generation drives lipotoxicity in women with polycystic ovary syndrome. *J Clin Endocrinol Metab*. 2017;102:3327-3339.
16. Barnard M, Quanson JL, Mostaghel E, Pretorius E, Snoep JL, Storbeck K-H. 11-Oxygenated androgen precursors are the preferred substrates for aldo-keto reductase 1C3 (AKR1C3): implications for castration resistant prostate cancer. *J Steroid Biochem Mol Biol*. 2018;183:192-201.
17. Paulukinas RD, Mesaros CA, Penning TM. Conversion of classical and 11-oxygenated androgens by insulin induced AKR1C3 in a model of human PCOS adipocytes. *Endocrinology*. 2022;163:bqac068.
18. Tomlinson JW, Walker EA, Bujalska IJ, et al. 11β-hydroxysteroid dehydrogenase type 1: a tissue-specific regulator of glucocorticoid response. *Endocr Rev*. 2004;25:831-866.
19. Gathercole LL, Lavery GG, Morgan SA, et al. 11β-hydroxysteroid dehydrogenase 1: translational and therapeutic aspects. *Endocr Rev*. 2013;34:525-555.
20. Gent R, du Toit T, Bloem LM, Swart AC. The 11β-hydroxysteroid dehydrogenase isoforms: pivotal catalytic activities yield potent C11-oxy C 19 steroids with 11βHSD2 favouring 11-ketotestosterone, 11-ketoandrostenedione and 11-ketoprogesterone biosynthesis. *J Steroid Biochem Mol Biol*. 2019;189:116-126.
21. Morgan SA, McCabe EL, Gathercole LL, et al. 11β-HSD1 is the major regulator of the tissue-specific effects of circulating glucocorticoid excess. *Proc Natl Acad Sci USA*. 2014;111:E2482-E2491.
22. Gregory S, Hill D, Grey B, et al. 11β-hydroxysteroid dehydrogenase type 1 inhibitor use in human disease—a systematic review and narrative synthesis. *Metabolism*. 2020;108:154246.

23. Tiganescu A, Hupe M, Uchida Y, Mauro T, Elias PM, Holleran WM. Topical 11β-hydroxysteroid dehydrogenase type 1 inhibition corrects cutaneous features of systemic glucocorticoid excess in female mice. *Endocrinology*. 2018;159:547-556.
24. Doig CL, Fletcher RS, Morgan SA, et al. 11β-HSD1 modulates the set point of brown adipose tissue response to glucocorticoids in male mice. *Endocrinology*. 2017;158:1964-1976.
25. Masuzaki H, Paterson J, Shinyama H, et al. A transgenic model of visceral obesity and the metabolic syndrome. *Science*. 2001;294:2166-2170.
26. Masuzaki H, Yamamoto H, Kenyon CJ, et al. Transgenic amplification of glucocorticoid action in adipose tissue causes high blood pressure in mice. *J Clin Invest*. 2003;112:83-90.
27. Kotelevtsev Y, Holmes MC, Burchell A, et al. 11beta-hydroxysteroid dehydrogenase type 1 knockout mice show attenuated glucocorticoid-inducible responses and resist hyperglycemia on obesity or stress. *Proc Natl Acad Sci USA*. 1997;94:14924-14929.
28. Hermanowski-Vosatka A, Balkovec JM, Cheng K, et al. 11β-HSD1 inhibition ameliorates metabolic syndrome and prevents progression of atherosclerosis in mice. *J Exp Med*. 2005;202:517-527.
29. Morgan SA, Gathercole LL, Hassan-Smith ZK, Tomlinson J, Stewart PM, Lavery GG. 11β-HSD1 contributes to age-related metabolic decline in male mice. *J Endocrinol*. 2022;255:117-129.
30. Rege J, Garber S, Conley AJ, et al. Circulating 11-oxygenated androgens across species. *J Steroid Biochem Mol Biol*. 2019;190:242-249.
31. Walker BR, Connacher AA, Lindsay RM, Webb DJ, Edwards CRW. Carbenoxolone increases hepatic insulin sensitivity in man: a novel role for 11-oxosteroid reductase in enhancing glucocorticoid receptor activation. *J Clin Endocrinol Metab*. 1995;80:3155-3159.
32. Andrews RC, Rooyackers O, Walker BR. Effects of the 11 beta-hydroxysteroid dehydrogenase inhibitor carbenoxolone on insulin sensitivity in men with type 2 diabetes. *J Clin Endocrinol Metab*. 2003;88:285-291.
33. Sandeep TC, Andrew R, Homer NZM, Andrews RC, Smith K, Walker BR. Increased in vivo regeneration of cortisol in adipose tissue in human obesity and effects of the 11beta-hydroxysteroid dehydrogenase type 1 inhibitor carbenoxolone. *Diabetes*. 2005;54:872-879.
34. Rosenstock J, Banarer S, Fonseca VA, et al. The 11-beta-hydroxysteroid dehydrogenase type 1 inhibitor INCB13739 improves hyperglycemia in patients with type 2 diabetes inadequately controlled by metformin monotherapy. *Diabetes Care*. 2010;33:1516-1522.
35. Feig PU, Shah S, Hermanowski-Vosatka A, et al. Effects of an 11β-hydroxysteroid dehydrogenase type 1 inhibitor, MK-0916, in patients with type 2 diabetes mellitus and metabolic syndrome. *Diabetes Obes Metab*. 2011;13:498-504.
36. Shah S, Hermanowski-Vosatka A, Gibson K, et al. Efficacy and safety of the selective 11β-HSD-1 inhibitors MK-0736 and MK-0916 in overweight and obese patients with hypertension. *J Am Soc Hypertens*. 2011;5:166-176.
37. Heise T, Morrow L, Hompesch M, et al. Safety, efficacy and weight effect of two 11β-HSD1 inhibitors in metformin-treated patients with type 2 diabetes. *Diabetes Obes Metab*. 2014;16:1070-1077.
38. Yadav Y, Dunagan K, Khot R, et al. Inhibition of 11β-hydroxysteroid dehydrogenase-1 with AZD4017 in patients with nonalcoholic steatohepatitis or nonalcoholic fatty liver disease: a randomized, double-blind, placebo-controlled, phase II study. *Diabetes Obes Metab*. 2022;24:881-890.
39. Abbas A, Schini M, Ainsworth G, et al. Effect of AZD4017, a selective 11β-HSD1 inhibitor, on bone turnover markers in postmenopausal osteopenia. *J Clin Endocrinol Metab*. 2022;107:2026-2035.
40. Ajjan RA, Hensor EMA, Del Galdo F, et al. Oral 11β-HSD1 inhibitor AZD4017 improves wound healing and skin integrity in adults with type 2 diabetes mellitus: a pilot randomized controlled trial. *Eur J Endocrinol*. 2022;186:441-455.
41. Hardy RS, Botfield H, Markey K, et al. 11βHSD1 inhibition with AZD4017 improves lipid profiles and lean muscle mass in idiopathic intracranial hypertension. *J Clin Endocrinol Metab*. 2021;106:174-187.
42. Bianzano S, Nordaby M, Plum-Mörschel L, Peil B, Heise T. Safety, tolerability, pharmacodynamics and pharmacokinetics following once-daily doses of BI 187004, an inhibitor of 11 beta-hydroxysteroid dehydrogenase-1, over 28 days in patients with type 2 diabetes mellitus and overweight or obesity. *Diabetes Obes Metab*. 2023;25:832-843.
43. O'Reilly MW, Glisic M, Kumarendran B, et al. Serum testosterone, sex hormone-binding globulin and sex-specific risk of incident type 2 diabetes in a retrospective primary care cohort. *Clin Endocrinol*. 2019;90:145-154.
44. Fauser BCJM, Tarlatzis F, Chang A, et al. Revised 2003 consensus on diagnostic criteria and long-term health risks related to polycystic ovary syndrome (PCOS). *Hum Reprod*. 2004;19:41-47.
45. Legro RS, Arslanian SA, Ehrmann DA, et al. Diagnosis and treatment of polycystic ovary syndrome: an endocrine society clinical practice guideline. *J Clin Endocrinol Metab*. 2013;98:4565-4592.
46. McCartney CR, Marshall JC. Polycystic ovary syndrome. *N Engl J Med*. 2016;375:54-64.
47. Legro RS, Kunselman AR, Dodson WC, Dunaif A. Prevalence and predictors of risk for type 2 diabetes mellitus and impaired glucose tolerance in polycystic ovary syndrome: a prospective, controlled study in 254 affected women. *J Clin Endocrinol Metab*. 1999;84:165-169.
48. Randeva HS, Tan BK, Weickert MO, et al. Cardiometabolic aspects of the polycystic ovary syndrome. *Endocr Rev*. 2012;33:812-841.
49. Jones H, Sprung VS, Pugh CJA, et al. Polycystic ovary syndrome with hyperandrogenism is characterized by an increased risk of hepatic steatosis compared to nonhyperandrogenic PCOS phenotypes and healthy controls, independent of obesity and insulin resistance. *J Clin Endocrinol Metab*. 2012;97:3709-3716.
50. Rocha ALL, Faria LC, Guimarães TCM, et al. Non-alcoholic fatty liver disease in women with polycystic ovary syndrome: systematic review and meta-analysis. *J Endocrinol Investig*. 2017;40:1279-1288.
51. Cai J, Wu CH, Zhang Y, et al. High-free androgen index is associated with increased risk of non-alcoholic fatty liver disease in women with polycystic ovary syndrome, independent of obesity and insulin resistance. *Int J Obes*. 2017;41:1341-1347.
52. Kumarendran B, O'Reilly MW, Manolopoulos KN, et al. Polycystic ovary syndrome, androgen excess, and the risk of nonalcoholic fatty liver disease in women: a longitudinal study based on a United Kingdom primary care database. *PLoS Med*. 2018;15:e1002542.

53. Matsuura K, Shiraishi H, Hara A, et al. Identification of a principal mRNA species for human 3alpha-hydroxysteroid dehydrogenase isoform (AKR1C3) that exhibits high prostaglandin D2 11-ketoreductase activity. *J Biochem*. 1998;124:940-946.
54. Pfaffl MW. A new mathematical model for relative quantification in real-time RT-PCR. *Nucleic Acids Res*. 2001;29:e45.
55. Willems E, Leyns L, Vandesompele J. Standardization of real-time PCR gene expression data from independent biological replicates. *Anal Biochem*. 2008;379:127-129.
56. Guan H, Yang K. RNA isolation and real-time quantitative RT-PCR. *Methods Mol Biol*. 2008;456:259-270.
57. Quanson JL, Stander MA, Pretorius E, Jenkinson C, Taylor AE, Storbeck K-HH. High-throughput analysis of 19 endogenous androgenic steroids by ultra-performance convergence chromatography tandem mass spectrometry. *J Chromatogr B Anal Technol Biomed Life Sci*. 2016;1031:131-138.
58. Schiffer L, Shaheen F, Gilligan LC, et al. Multi-steroid profiling by UHPLC-MS/MS with post-column infusion of ammonium fluoride. *J Chromatogr B Anal Technol Biomed Life Sci*. 2022;1209:123413.
59. Foster MA, Taylor AE, Hill NE, et al. Mapping the steroid response to major trauma from injury to recovery: a prospective cohort study. *J Clin Endocrinol Metab*. 2020;105:925-937.
60. Chadwick CA, Owen LJ, Keevil BG. Development of a method for the measurement of dehydroepiandrosterone sulphate by liquid chromatography-tandem mass spectrometry. *Ann Clin Biochem*. 2005;42:468-474.
61. Shackleton CHL. Profiling steroid hormones and urinary steroids. *J Chromatogr*. 1986;379:91-156.
62. Snaterse G, Mies R, van Weerden WM, et al. Androgen receptor mutations modulate activation by 11-oxygenated androgens and glucocorticoids. *Prostate Cancer Prostatic Dis*. 2022;26:293-301.
63. Scott JS, Bowker SS, Deschoolmeester J, et al. Discovery of a potent, selective, and orally bioavailable acidic 11β-hydroxysteroid dehydrogenase type 1 (11β-HSD1) inhibitor: discovery of 2-[(3S)-1-[5-(cyclohexylcarbamoyl)-6-propylsulfanylpyridin-2-yl]-3-piperidyl]acetic acid (AZD4017). *J Med Chem*. 2012;55:5951-5964.
64. Barnard L, Nikolaou N, Louw C, et al. The A-ring reduction of 11-ketotestosterone is efficiently catalysed by AKR1D1 and SRD5A2 but not SRD5A1. *J Steroid Biochem Mol Biol*. 2020;202:105724.
65. Davio A, Woolcock H, Nanba AT, et al. Sex differences in 11-oxygenated androgen patterns across adulthood. *J Clin Endocrinol Metab*. 2020;105:e2921-e2929.
66. Handelsman DJ, Cooper ER, Heather AK. Bioactivity of 11 keto and hydroxy androgens in yeast and mammalian host cells. *J Steroid Biochem Mol Biol*. 2022;218:106049.
67. O'Reilly MW, Taylor AE, Crabtree NJ, et al. Hyperandrogenemia predicts metabolic phenotype in polycystic ovary syndrome: the utility of serum androstenedione. *J Clin Endocrinol Metab*. 2014;99:1027-1036.
68. Schiffer L, Kempegowda P, Arlt W, O'Reilly MW. MECHANISMS IN ENDOCRINOLOGY: the sexually dimorphic role of androgens in human metabolic disease. *Eur J Endocrinol*. 2017;177:R125-R143.
69. Kempegowda P, Melson E, Manolopoulos KN, Arlt W, O'Reilly MW. Implicating androgen excess in propagating metabolic disease in polycystic ovary syndrome. *Ther Adv Endocrinol Metab*. 2020;11:2042018820934319.
70. Paulukinas RD, Penning TM. Insulin-induced AKR1C3 induces fatty acid synthase in a model of human PCOS adipocytes. *Endocrinology*. 2023;164:bqad033.
71. Oda S, Ashida K, Uchiyama M, et al. An open-label phase I/IIa clinical trial of 11β-HSD1 inhibitor for Cushing's syndrome and autonomous cortisol secretion. *J Clin Endocrinol Metab*. 2021;106:E3865-E3880.
72. Prete A, Subramanian A, Bancos I, et al. Cardiometabolic disease burden and steroid excretion in benign adrenal tumors: a cross-sectional multicenter study. *Ann Intern Med*. 2022;175:325-334.
73. Zhu L, Hou M, Sun B, et al. Testosterone stimulates adipose tissue 11beta-hydroxysteroid dehydrogenase type 1 expression in a depot-specific manner in children. *J Clin Endocrinol Metab*. 2010;95:3300-3308.
74. Pivonello R, Menafra D, Riccio E, et al. Metabolic disorders and male hypogonadotropic hypogonadism. *Front Endocrinol (Lausanne)*. 2019;10:345.
75. Kroon J, Pereira AM, Meijer OC. Glucocorticoid sexual dimorphism in metabolism: dissecting the role of sex hormones. *Trends Endocrinol Metab*. 2020;31:357-367.
76. Ruiz D, Padmanabhan V, Sargis RM. Stress, sex, and sugar: glucocorticoids and sex-steroid crosstalk in the sex-specific misprogramming of metabolism. *J Endocr Soc*. 2020;4:bvaa087.
77. Kaikaew K, Grefhorst A, Visser JA. Sex differences in brown adipose tissue function: sex hormones, glucocorticoids, and their crosstalk. *Front Endocrinol (Lausanne)*. 2021;12:357.
78. Markey K, Mitchell J, Botfield H, et al. 11β-hydroxysteroid dehydrogenase type 1 inhibition in idiopathic intracranial hypertension: a double-blind randomized controlled trial. *Brain Commun*. 2020;2:fcz050.
79. Shifren JL. Androgen deficiency in the oophorectomized woman. *Fertil Steril*. 2002;77:60-62.
80. Stanczyk FZ, Chaikittisilpa S, Sriprasert I, Rafatnia A, Nadadur M, Mishell DR. Circulating androgen levels before and after oophorectomy in premenopausal and postmenopausal women. *Climacteric*. 2019;22:169-174.
81. Hardy RS, Zhou H, Seibel MJ, Cooper MS. Glucocorticoids and bone: consequences of endogenous and exogenous excess and replacement therapy. *Endocr Rev*. 2018;39:519-548.

SUPPORTING INFORMATION

Additional supporting information can be found online in the Supporting Information section at the end of this article.

How to cite this article: Schiffer L, Oestlund I, Snoep JL, et al. Inhibition of the glucocorticoid-activating enzyme 11β-hydroxysteroid dehydrogenase type 1 drives concurrent 11-oxygenated androgen excess. *The FASEB Journal*. 2024;38:e23574. doi:10.1096/fj.202302131R